SETSCI conference proceedings

SETSCI Conference Proceedings

9, 197-202, 2019

4th International Symposium on Innovative Approaches in Engineering and Natural Sciences

November 22-24, 2019, Samsun, Turkey

https://doi.org/10.36287/setsci.4.6.058

2687-5527/ © 2019 The Authors. Published by SETSCI

ISAS WINTER - 2019

A New Method for Diagnostics of Faults of Three-phase Squirrel Cage Asynchronous Motor

Osman Zeki Erbahan[1], İbrahim Aliskan[1*], Rıdvan Keskin[1+]

[1]*Bülent Ecevit University*
[*]*Corresponding Author:ialiskan@beun.edu.tr*
[+]*Speaker:ridvan.keskin@beun.edu.tr*
Presentation/Paper Type: Oral/Full Paper

***Abstract*—Asynhronous motors are the most widely used motors in the industry. They are found in every point of production lines since they are in a very advantageous structure. It is desirable to detect faults of these motors in a quick and easy way. In this article, the determination of rotor fault of asynchronous motors by acoustic measurements is investigated. Ac driver, motor breaking unit and microphone were used in the test circuit alongside a healty and faulty motor. Changes in the time domain using the matlab software, changes in the frequency domain were obtained by making fast fourier transform. FFT differences in sound files optained from operation in different speed and torque values of motors with rubost and broken rotor bar motors were detected and interpreted.**

Keywords: *Motor Fault, Fast Fourier Transform, Matlab*

I. INTRODUCTION

Asynchronous motors are the most commonly used electrical equipment in the industry and cause the most electricity consumption. Turkey Statistical Institutions (TSI) 92013 in publications that Turkey overall electricity consumption reported in at 47.1% for the industry of electric energy in Turkey, 67% of the motors of the electricity consumed in industry, 91% of the electricity consumed in the motor 0.75 to 1000 kW power range is consumed in motors and 87% of these motors can be said to be asynchronous motors. These values show that asynchronous motors used in industry cover about 25% of the total energy consumption [1]. Failure of such widely used motors leads to production losses. Proactive maintenance is required to detect failure in advance to prevent loss of production. By examining many important methods in this subject, a study on the diagnosis of the failure of squirrel cage asynchronous motors will be transferred. In the literature review; Failure rates of the components of the squirrel cage asynchronous motor; bearing errors were determined as 40%, stator errors as 36% [2]. Bearing errors and stator faults have been found in the field of application by suggesting various solution methods by carrying out numerous studies [3] [4]. It has been determined that malfunctions in asynchronous motors occur between 5% and 10% of fracture of rotor rods [5]. However, an easy and reliable solution for the diagnosis of rotor faults methods and measuring apparatus has not reached the usable stage yet. Therefore, it was decided to carry out studies on this subject. Fault detection in single-phase asynchronous motor has been examined using acoustic measurement method [6], similar studies have been performed in fault detection in synchronous motors [7] [8], many studies have been made in detection of faults in motors using acoustic measurement and different algorithms have been successfully applied in fault detection [9] [10]. Rotor fracture fault detection in drive systems can detect faulty rotor rod failure for asynchronous motors in both open and closed loop drives [11]. Another proposed method for rotor fracture detection is the Hilbert transform of the phase current and the spectral analysis of this conversion module with FFT [12]. In a different study examining stator and rotor failures, Fourier transform based motor current signature analysis was used to extract the properties of broken rotor rod. For the stator failures, a feature extraction process based on park vector transformation and principal component analysis was performed. A feedforward artificial neural network was used to realize the model [13]. The results of the study using the envelope analysis method show that statistical analysis methods can be used in the investigation and detection of rotor faults in squirrel-cage asynchronous motors [14].

Considering the literature, we noticed that acoustic signals could be utilized to detect rotor fault detection in induction motors. Accordingly, three phase squirrel cage asynchronous motor for the detection of fractures in the rotor rod test circuit detection process has been completed, 2 GAMAK motors to be used in the circuit has been provided. ABB brand ac drive is provided for speed adjustment. A condenser microphone is provided for acoustic measurement. The block diagram of the test is given in Figure 1.

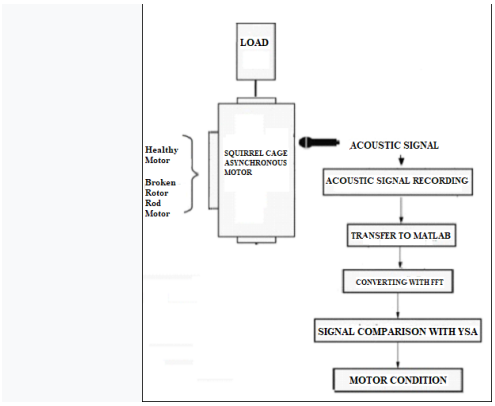


Figure 1. *Block Diagram of the Test Circuit of the Study*

Acoustic measurements were made at various speeds and loads in the healthy motor and their FFT was made via Matlab. FFT values were determined by making similar measurements in this motor by creating a rod error in the rotor of the second motor.

The rest of the paper is organized as follows: Section II explains the test circuit, the generation of rotor rod failure, measurements and data tables obtained from the test studies. Section III gives information about artificial neural networks and rotor fault detection studies. The paper is concluded by Section IV.

II. TEST STUDIES

A. Testing Equipments

Asynchronous Motor; the winding resistance of asynchronous motors can be obtained experimentally as a result of the idle test and short circuit test. Accordingly, the T-shaped equivalent circuit given in Figure 2 is obtained. The right side of the equivalent circuit shows the rotor and the left side shows the stator. The set resistance seen in the equivalent circuit shows the ohmic resistance changing with the shift in the rotor equivalent circuit [15] [16] [17].

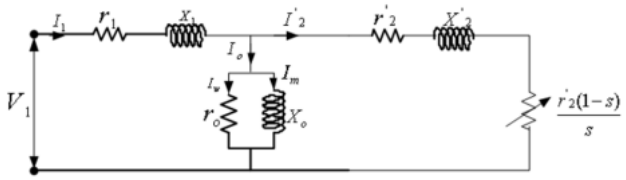


Figure 2. *T-shaped equivalent diagram of the asynchronous motor*

The rotational speed of the rotor of the motor (n_2) is smaller than the rotational speed of the magnetic field (n_1) generated by the stator. This difference is called shift (s).

$$s = \frac{n_1 - n_2}{n_1} \quad (1)$$

$n_1 = \frac{f_1 \cdot 60}{p}$, In the equation; p is the pole pair number of the motor.

n_2 is the rotational speed of the motor and the value indicated on the motor nameplate.

The formula that relates the torque of the motor to the rotor resistance;

$$M = \frac{m_1 U_1^2 r_2'}{s.w_1\left[\left(r_1+\frac{c_1 r_2'}{s}\right)^2+(x_1+c_1 x_2')^2\right]} \quad [N.m] \quad (2)$$

Here the value of c_1 should be taken as approximately 1+ (x_1 / x_m). For motors with a power rating above 1 kW, this value can be around 1.04 to 1.08 [18]. In this study asynchronous motors GAMAK brand AGM71 4a model 3 phase 0.25kW 1390 rpm, 380V AC, 0.8A two squirrel cage asynchronous motors were used. Figure 3 gives the pictures of the motors used.



Figure 3. *GAMAK AGM71 4a, used motor*

AC Drive; in order to perform acoustic measurement of the motor at various speeds in the test circuit, a ABB brand ACS150 model 0.37kW drive was used as AC driver. Figure 4 shows the pictures of the drive used.



Figure 4. *ABB AC Driver 0.37kW*

Braking Unit; Braking test unit in ZBEU Electrical Machine Laboratory was used for acoustic measurement of the

motor at various loads. The braking unit and the controller of the braking unit are shown in Figure 5.

(a)  (b) 

Figure 5. (a) *Breaking Unit* ***(b)*** *Breaking Unit Controller*

Microphone; TRUST brand condenser type microphone is used for acoustic measurements. The sensitivity range of the microphone is between 100Hz and 10kHz. Figure 6 shows the microphone image.



Figure 6. *TRUST Brand Microphone*

Generating Rotor Error; when the torque curves of squirrel cage motors are examined according to rotor resistance, it is observed that when the rotor resistance increases, the torque curves shift to the left and the initial torque values increase. Rotor rod fractures increase rotor resistance. In this way, it causes the maximum torque point to shift to the left in the torque curve of the motor. This change in rotor resistance can be captured by the change in torque. According to this change value, the number of broken rotor rods can be determine.

If the rotor rods of the motor break, the starting of the motor becomes longer and harder and motor noise changes. The ammeter pointer, which indicates the stator current, oscillates at the rotor frequency when it is switched to continuous operation. If a cage failure is not detected in time, the cage, or even the rotor hair package, may need to be completely replaced [19].

After the rotor was removed from the motor, a 2mm diameter hole was drilled from the point where the aluminum short circuit rods of the rotor were broken and the cracked rod failure was formed. Figure 7 shows the hole drilled into the rotor.

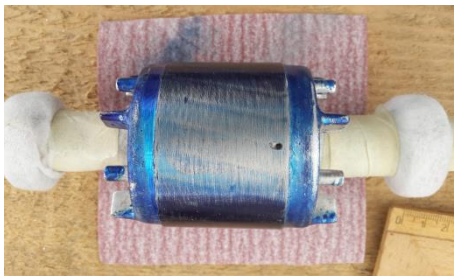


Figure 7. *Single rotor rod damage (the hole diameter 2 mm)*

B. Test Measurements

The AC driver used for the motor supplied with 3-phase 380V voltage is connected to the mains. The motor is connected to the braking unit with the appropriate coupling and coupled to the motor shaft in a way that does not generate vibration. The microphone is located near the shaft of the motor. The microphone was connected to the computer and the laptop computer and audio files in *.m4a format were recorded according to the load and speed values indicated in Tables 1 and 2.

When controlling the motor speed with the drive, the load change is made in Nm via the Braking controller. The motor is set to 0% (no load), 25%, 50%, 75%, 100% and 125% according to the nominal torque. They are applied to healthy and rod failure motors. The audio files for these cases are recorded. Figure 8 shows the picture of the test circuit.



Figure 8. *Test circuit of the study*

Table 1. *Sound files obtained at different speeds and loads of the healthy motor*

Torque **Speed**	**0%** *(0Nm)*	**25%** *(0,42Nm)*	**50%** *(0,85Nm)*	**75%** *(1,28Nm)*	**100%** *(1,71Nm)*	**125%** *(2,14Nm)*
25% 347rpm	Ses1	Ses6	Ses11	Ses16	Ses21	Ses26
50% 696rpm	Ses2	Ses7	Ses12	Ses17	Ses22	Ses27
75% 1042rpm	Ses3	Ses8	Ses13	Ses18	Ses23	Ses28
90% 1251rpm	Ses4	Ses9	Ses14	Ses19	Ses24	Ses29

100% 1390rpm	Ses5	Ses10	Ses15	Ses17	Ses25	Ses30

Table 2. *Sound files obtained at different speeds and loads of the motor with a single fracture in the rotor rod*

Torque **Speed**	**0%** *(0Nm)*	**25%** *(0,42Nm)*	**50%** *(0,85Nm)*	**75%** *(1,28Nm)*	**100%** *(1,71Nm)*	**125%** *(2,14Nm)*
25% 347rpm	rses1	rses6	rses11	rses16	rses21	rses26
50% 696rpm	rses2	rses7	rses12	rses17	rses22	rses27
75% 1042rpm	rses3	rses8	rses13	rses18	rses23	rses28
90% 1251rpm	rses4	rses9	rses14	rses19	rses24	rses29
100% 1390rpm	rses5	rses10	rses15	rses20	rses25	rses30

The following software is used to evaluate the audio files recorded by running the motor with Matlab and to obtain FFT. The recorded sound wave values of the motor are normalized. Then, filtering was applied by applying **windowing method** [6].

In this method;

1. [y,fs] = audioread('ses6.wma') sound wave was divided into 80 tracks at the intervals given below . yy1=y(1:11025),yy2=y(11026:22050), yy3=y(22051:33075),…
2. These pieces were added and divided into 80 pieces.

   yy= (yy1+yy2+….+yy80)/80
3. FFT values of the obtained new sound wave were obtained.

The spectra obtained after evaluating the **rses6.m4a** file specified by Matlab as an example are given in Figures 9, 10 and 11 below.

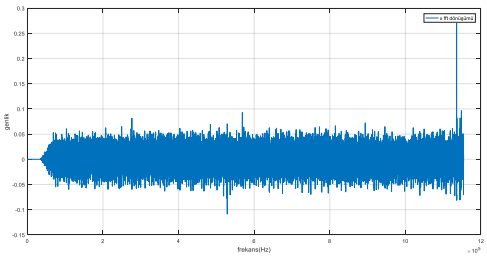


Figure 9. *Recorded 10 second change of rses6.m4a sound wave*

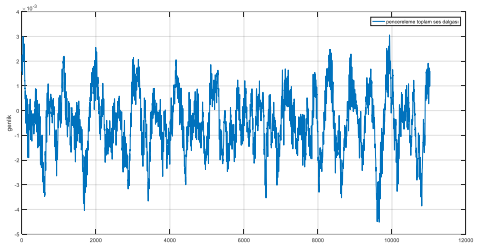


Figure 10. *Change of total sound wave obtained after windowing method is applied*

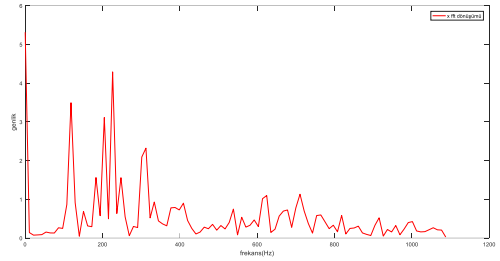


Figure 11. Spectral change obtained employing FFT transformation after windowing

25% torque (0.425Nm) and speed 25% (347rpm) rses6.m4a audio file of the broken rotor motor is processed in Matlab software and spectrum outputs are given below.

```
[y,fs] = audioread('rses6.m4a');
y = resample(y,100000,fs);
yy5=y(44101:55125);
yy=(yy1+yy2+yy3+yy4+yy5+…)/80;
figure;
subplot(2,2,1);
plot(yy5);
grid;
legend('yy5');
ylabel('genlik');
N=4096;
freq = linspace(0,fs,N);
subplot(2,2,2);
plot(yy);
grid;
ylabel('genlik');
legend('yy toplam');
subplot(2,2,3);
F = fft(yy);
```

```
maxFreq = N/2;

plot(freq(1:maxFreq),(abs(F(1:maxFreq))),'r');

grid;
```

In this study, acoustic measurements were performed on the motors which were damaged and the rods of the rotor were damaged and these recordings were completed at various speeds and loads. The variation of the FFT spectrum of the healthy and damaged motor operating at idle maximum speed is shown in Figure 12.

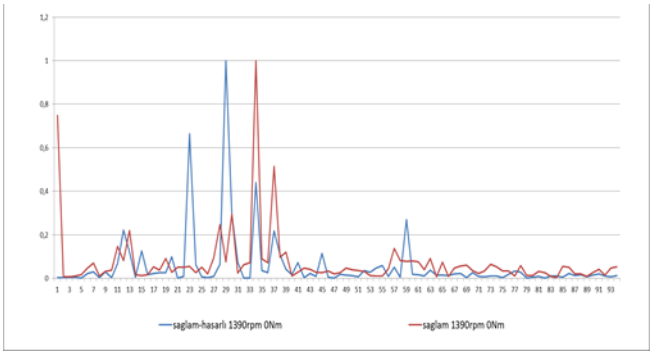


Figure 12. *Healthy-damaged difference fft spectrum at the same speed and torque as the fft spectrum at 0% torque (0Nm) and 100% rpm (1390rpm) of the motor in healthy construction*

FFT results obtained from audio files are given in Table 3 for the sampled values. If Table 3 is examined, it is observed that there is a difference in the amplitudes between FFT results of the healthy motor and FFT results of the damaged motors.

Table 3. *Comparison of sampling FFT of sound files taken when operating at 0% torque (no load) and 100% rated speed of the motor with a single broken rotor rod and a healthy motor*

Frequency *(Hz)*	12	23	29	34	37	45	59
Amplitude (Sağlam)	0,08	0,05	0,07	1	0,51	0,02	0,07
Amplitude (Hasarlı)	0,22	0,66	1	0,43	0,21	0,11	0,27

III. PREDICTION BY ARTIFICIAL NEURAL NETWORKS(ANN)

A. Two-layer feedforward neural networks, including latent neurons and linear output neurons, can well adapt and solve multi-dimensional imaging problems with latent layers containing sufficient numbers of neurons. The network is trained with the Levenberg-Marquardt back propagation algorithm (trainlm).

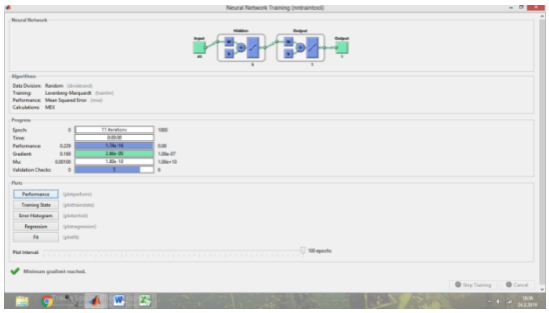


Figure 13. *Two-layer feedforward network structure*

Figure 13 shows the feed forward structure of the model. There are 54 explanatory variables in the Input section. In the Hidden Layer section, the weight coefficients (w1, w2,... wn) and the treshold value (b1, b2,... bn) are determined using hyperbolic tangent function. For the model being analyzed, these weight and variable coefficients are processed in the output layer within the framework of linear function. Then, the output is estimated as output. The number of neurons in the latent layer is taken into account in determining the model performance. For model performance, one hidden layer with 5-10 neurons were tested. The best model performance is achieved when the R2 value approaches 1 and the MSE approaches 0.

Table 4 reflects the results of the model analysis using forward feed back propagation algorithm in artificial neural networks. The model was run with learning, validation and testing. Accordingly, the number of neurons in the hidden layer and the learning rates were changed for each learning-validation-testing process. In this respect, R2 and MSE were used as important performance indicators in terms of model results. In the established models, 54 data were used for learning, validation and testing at different rate.

Table 4. *Rates-Neuron Numbers and Prediction Results Table*

Sampling Rates	**50-25-25 (Learning/Validation/Test)**			
Sampling Rates	26-14-14			
Hidden	10		5	
Output	1			
	R2	MSE	R2	MSE
Learning	0,99259	0,00547	0,98922	0,00691
Validation	0,68987	0,18205	0,61617	0,12902
Test	**0,84008**	**0,06701**	0,69756	0,01360

Sampling Rates	**60-20-20 (Learning/Validation/Test)**			
Sampling Rates	32-11-11			
Hidden	10		5	
Output	1			
	R2	MSE	R2	MSE
Learning	0,99360	0,00089	0,97715	0,02690
Validation	0,82031	0,11901	0,68206	0,19423
Test	0,78560	0,07720	0,79428	0,09602

Sampling Rates	**75-15-15 (Learning/Validation/Test)**			
Sampling Rates	38-8-8			
Hidden	10		5	
Output	1			
	R2	MSE	R2	MSE
Learning	0,99090	0,00774	**0,99499**	**0,00235**

Validation	0,86644	0,08590	0,83821	0,08485
Test	0,83999	0,13750	0,82765	0,00775

When Table 4 is evaluated, the model with the two-layer feed back feed-back algorithm used the input of 54 explanatory variables, 26 data with 10 neurons in the hidden layer for learning, 14 data for validation and 14 data for the test showed the best performance and MSE = 0.06701 and R2 = 0.84008. ANN model was run with Matlab 7.6.0 (R2016a) package program. The maximum number of iterations was determined as 1000 and the number of iterations reached from 1000 to 11 iterations.

IV. RESULTS

As a result, considering the values given in Table 3 in the FFT values of the healthy and rotor broken motor, it is possible to detect the fractures occurring in the rotor rods of the motor by acoustic measurements. In this table, it is observed that the amplitude values of 0.05 and 0.07 during 23 Hz and 29 Hz of the motor operating at idle nominal speed increase more than 10 times like broken rotor rod motor values of 0.66 and 1.0. The reason for this difference is the change in motor torque due to the change in rotor resistance.

In the ANN application, when the two-layer forward feed back propagation algorithm was used, as shown in Table 4, the model using 26 data for 10 neurons in the hidden layer for learning, 14 data for validation and 14 data for test showed the best performance and MSE = 0.06701 and R2 = 0.84008.

.

INFORMATİON

The informations are hidden.

REFERENCES

[1] Türkiye İstatistik Kurumu, Net Elektrik Tüketiminin Sektörlere Göre Dağılımı 2013, http://www.tuik.gov.tr/

[2] R. G. Smiley, "Using line current to diagnose faults in induction motors", Iron and Steel Engineer, ss. 23-25, 1992

[3] P.C.M. Lamim Filho, R. Pederiva ve J.N. Brto, "Detection of stator winding faults ın ınduction machines using flux and vibration anallysis", Mechanical Systems and Signal Processing, c. 42, s. 1-2, ss. 377-387, 2014

[4] A. Bellini, F. Filipetti ve C. Tassoni, "Advances in diagnostic techniques for induction machines", IEEE Trans. Ind. Electron. c. 5, s. 12, ss. 4109-4126, 2008

[5] S. Nandi, H. Tolyat ve X. Li, ''Condition monitoring and fault diagnosis of electrical motors a rewiev," IEEE Trans. Energy Convers., c. 20, s. 4, ss. 719-729, 2005

[6] A. Glowacz ve Z. Glowacz, "Diagnosis of stator faults of the single-phase induction motor using acoustic signal," Applied Acoustic, s. 17, ss. 20-27, 2017.

[7] A. Glowacz, "Recognition of acoustic signals of synchronous motors with the use of MoFS and selected classifiers," Measure. Sci. Rev. c. 15, s.415(4)ss. 167–175, 2015.

[8] A. Glowacz, "Fault diagnostics of acoustic signals of loaded synchronous motor using SMOFS-25-EXPANDED and selected classifiers" Tehnicki Vjesnik- Technical Gazette, c.23, s.5, ss. 1365–1372, 2016.

[9] E. Germen, M. Başaran, M. Fidan, "Sound based induction motor fault diagnosis using Kohonen self-organizing map" Mechanical Systems and Signal Processing Volume 46, Issue 1, Pages 45-58, 2014

[10] A. Alwodai, F. Gu and A. D. Ball, "A Comparison of Different Techniques for Induction Motor Rotor Fault Diagnosis" J. Phys, Conf. Ser. 364 012066, 2012

[11] D. Stankovic , Z. Zhang , I. Voloh , J. Vico , "Enhanced algorithm for motor rotor broken bar detection" 63rd Annual Conference for Protective Relay Engineers, 2010

[12] V. Sarkimaki , P. Rodriguez Detection of broken rotor rod malfunction in induction machine fed by frequency converter", IET Electric Power Applications Cilt: 11, Sayı: 7, 8, 1214 – 1223, 2017

[13] İ. Aydın, M. Karaköse , E. Akın, "Kırık Rotor Çubuğu ve Stator Arızalarının Teşhisinde Yapay Sinir Ağı Yaklaşımı", Erciyes Üniversitesi Fen Bilimleri Enstitüsü Dergisi 25 (1-2) 134 - 149 http://fbe.erciyes.edu.tr/ ISSN 1012-2354 1, 2009

[14] A. Ünsal, A. Kabul, "Asenkron Motor Rotor Arızalarının İstatiksel Analiz Yöntemi ile Değerlendirilmesi", Politeknik Dergisi,; 20 (2) : 283-289, 2017

[15] İ. Çolak, 'Elektrik makinaları 2 Asenkron Motorlar-Senkron Motorlar' Seçkin yayınları 4. Baskı, 2017

[16] A.İ., Çanakoğlu, A.G.,Yetkin, H. Temurtaş, M. Turan, 'Induction motor parameter estimation using metaheuristic methods', Research Artikel, Turkish Journal of Electrical Engineering & Computer Sciences (22), 1077-1192, 2014

[17] D. Lindemeyer, H.W. Dommel, A. Moshref, P. Kundur, 'An Induction Motor Parameter Estimation Method' Electrical Power and Energy Systems 23, pp 251-262, 2001

[18] A. N. Şerifoğlu, ' Elektrik Makinaları Transformatörler ve Asenkron Motorlar ' Cilt2 Nobel Yayınevi 2007

[19] W. Schuisky, İ. Çetin 'Elektrik Motörleri' 1. Kısım, Fatih Yayınevi, İstanbul, 1987